SLAC-PUB-2674
February 1981
(T/E)

INTERNAL SPIN STRUCTURE OF THE PROTON FROM HIGH-ENERGY POLARIZED e-p SCATTERING*

Vernon W. Hughes
Gibbs Laboratory, Physics Department
Yale University, New Haven, Connecticut 06520

G. Baum, M.R. Bergström, P.R. Bolton, J.E. Clendenin, N.R. DeBotton, S.K. Dhawan, R.A. Fong-Tom, Y.-N. Guo, V.-R. Harsh, K. Kondo, M.S. Lubell, C.-L. Mao, R.H. Miller, S. Miyashita, K. Morimoto, U.F. Moser, I. Nakano, R.F. Oppenheim, D.A. Palmer, L. Panda†, W. Raith, N.Sasao, K.P. Schüler, M.L. Seely, J. Sodja, P.A. Souder, S.J. St. Lorant, K. Takikawa, M. Werlen

University of Bern, Switzerland; University of Bielefeld, Germany; Institute of High Energy Physics, Beijing, China; National Laboratory for High Energy Physics, KEK, Tsukuba, Japan; Kyoto University, Japan; SACLAY, Saclay, France; Stanford Linear Accelerator Center, Stanford, California; University of Tsukuba, Ibaraki, Japan; and Yale University, New Haven, Connecticut.

ABSTRACT

A review is given of our experimental knowledge of the spin dependent structure functions of the proton, which is based on inclusive high energy scattering of longitudinally polarized electrons by longitudinally polarized protons in both the deep inelastic and resonance regions, and includes preliminary results from our most recent SLAC experiment. Implications for scaling, sum rules, models of proton structure, and the hyperfine structure interval in hydrogen are given. Possible future directions of research are indicated.

INTRODUCTION

The internal spin structure of the proton (and neutron), or the spin dependent structure functions, is a central aspect of nucleon structure. Knowledge of this spin structure is important to the development and testing of theories and models of nucleon structure, as well as to the understanding of spin dependent phenomena involving hadrons, such as polarized hadron-hadron scattering at high energies.

Spin dependent structure functions of the proton can be studied by high energy e-p scattering of polarized electrons by polarized protons,[1] which is especially interesting in the deep inelastic regime where the impulse approximation of e^- scattering from the constituent partons or quarks is valid. However, resonance region scattering at lower energy and momentum transfer is also informative about proton spin structure. Figure 1 indicates the kinematics of polarized e-p inclusive scattering in which the momentum and scattering angle of the scattered electron are measured. The e-p asymmetry, A, which is the normalized difference between the differential scattering cross sections with electron and proton spins anti-parallel and parallel, is the quantity measured. Tables 1 and 2 give definitions and relations for the quantities relevant to asymmetry. Thus far only inclusive scattering with longitudinal electron and proton spins has been measured.

* Work supported in part by the Department of Energy under contracts DE-AC03-76SF00515 and DE-AC02-76ER03075, and by John Simon Guggenheim Memorial Foundation Fellowship, 1978-1979, to VWH.

† Deceased.

(Invited paper presented at the 1980 International Symposium on High Energy Physics with Polarized Beams and Polarized Targets, Lausanne, Switzerland, September 25 - October 1, 1980.)

$q = (p - p')$

$Q^2 = -q^2 = 4EE' \sin^2 \frac{\theta}{2}$

$\tau = Q^2/4M^2$

$\nu = E - E'$

$\omega = 2M\nu/Q^2$

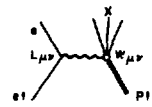

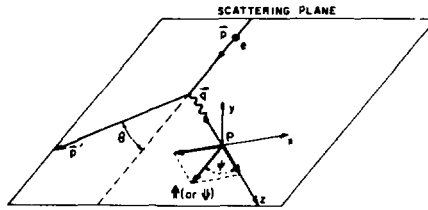

Fig. 1. Kinematics for the scattering of longitudinally polarized electrons by longitudinally polarized protons.

$$\frac{d^2\sigma}{d\Omega dE'} = \left(\frac{d\sigma}{d\Omega}\right)_{MOTT} L_{\mu\nu} W_{\mu\nu} \qquad \left(\frac{d\sigma}{d\Omega}\right)_{MOTT} = \frac{\alpha^2}{4E^2} \frac{\cos^2\frac{\theta}{2}}{\sin^4\frac{\theta}{2}}$$

$$A \equiv \frac{\frac{d^2\sigma}{d\Omega dE'}(\uparrow\downarrow) - \frac{d^2\sigma}{d\Omega dE'}(\uparrow\uparrow)}{\frac{d^2\sigma}{d\Omega dE'}(\uparrow\downarrow) + \frac{d^2\sigma}{d\Omega dE'}(\uparrow\uparrow)}$$

2 - 81
4028A1

(CROSS SECTION AND ASYMMETRY

$$\frac{d^2\sigma}{d\Omega dE'} = \left(\frac{\alpha^2\cos^2\frac{\theta}{2}}{4E^2\sin^4\frac{\theta}{2}}\right)\left[W_2 + 2\tan^2\frac{\theta}{2} W_1 \pm 2\tan^2\frac{\theta}{2} \frac{E+E'\cos\theta}{M} \right.$$
$$\left. \pm \frac{2E'}{M}\tan^2\frac{\theta}{2}\sin^2\frac{\theta}{2}\right]$$

$$\frac{d^2\sigma}{d\Omega dE'} = \left(\frac{d\sigma}{d\Omega}\right)_M \left(\epsilon(1+R)\frac{1}{(1+\nu^2/Q^2)}\right) W_2 \left[1 \pm \epsilon P_B P_T (1-\epsilon^2)^{1/2}\cos\phi A_1\right.$$
$$\left. \pm \left[2\epsilon(1-\epsilon)\right]^{1/2} \sin\phi A_2\right]$$

$$\epsilon = \left[1 + 2\left(1+\nu^2/Q^2\right)\tan^2\frac{\theta}{2}\right]^{-1}$$

$$D = \sigma_L/\sigma_T, \quad \sigma_T = (\sigma_{1/2} + \sigma_{3/2})/2$$

$$A = \frac{\sigma\uparrow\downarrow - \sigma\uparrow\uparrow}{\sigma\uparrow\downarrow + \sigma\uparrow\uparrow}$$

$$A = D(A_1 + \eta A_2)$$

$$D = \frac{1 - \epsilon E'/E}{\epsilon(1+\epsilon R)} = \frac{(1-\epsilon^2)^{1/2}\cos\phi}{(1+\epsilon R)}$$

$$\eta = \frac{\epsilon(Q^2)^{1/2}}{E - E'\epsilon} = \left(\frac{2\epsilon}{1+\epsilon}\right)^{1/2}\tan\phi = \tan\phi$$

$$A_1 = \frac{\sigma_{1/2} - \sigma_{3/2}}{\sigma_{1/2} + \sigma_{3/2}}$$

$$A_2 = \frac{2\sigma_{\perp}}{\sigma_{1/2} + \sigma_{3/2}}$$

$|A_1| \leq 1; \quad |A_2| \leq \sqrt{R}$ (POSITIVITY LIMITS)

2 - 81
4028A16

Table 1. Cross section and asymmetry for scattering of longitudinally polarized electrons by longitudinally polarized protons.

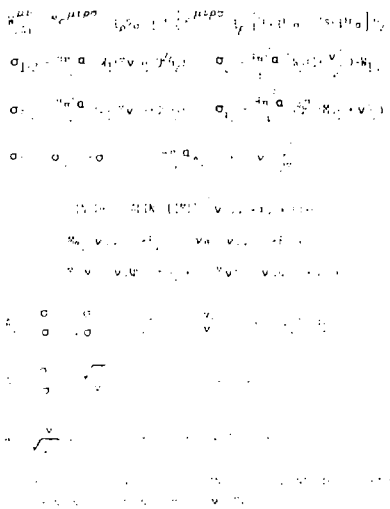

Table 2. Some definitions and relations of structure functions and asymmetries.

YALE-SLAC EXPERIMENT

The Yale-SLAC experiments to measure A were initiated in 1971 with the approval of the SLAC E80 experiment. All the results from this experiment have been published.[2-5] Data-taking for a second experiment SLAC E130 was completed in April, 1980, and preliminary results have been reported.[6]

The experimental technique for SLAC E80 has been described in our above publications. The polarized electron source[7] is based on photoionization of spin polarized Li atoms, and the polarized proton target[8] is based on dynamic nuclear polarization using the hydrocarbon butanol. The SLAC 8 GeV/c spectrometer was used as the detector in SLAC E80. The principal new feature of SLAC E130 was the use of a new large acceptance spectrometer. The experimental set-up for SLAC E130 is shown in Fig. 2. The new spectrometer is shown in Fig. 3. It utilizes two large dipole magnets (B20l and B8i) and a detector system which consists of a 1 m diameter × 4 m long N_2 gas Cerenkov counter, a 4000 wire PWC system, a

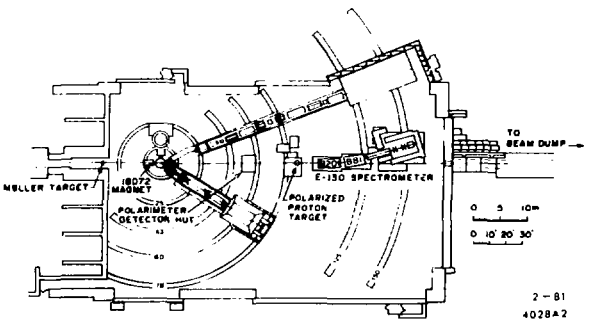

Fig. 2. SLAC E130 experimental set-up in end station A.

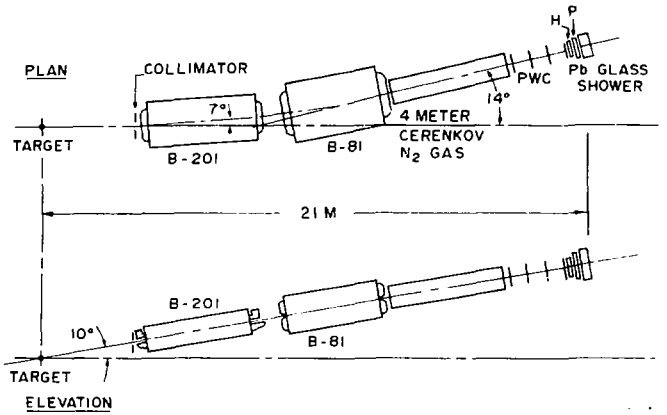

Fig. 3. SLAC E130 spectrometer.

hodoscope, and a segmented lead glass shower counter. The spectrometer may cover momenta up to 18 GeV/c, and its acceptance $\int d\Omega\, dp/p$ is 0.3 msr with the total momentum acceptance $\Delta p/p$ being about 50%. The momentum resolution of the spectrometer $\delta p/p$ is better than ±1%. For the measurement of the electron polarization P_e by Møller scattering,[9] a new feature was the detection of the two scattered electrons in coincidence. Counting rates and various sources of systematic errors in SLAC E130 are indicated in Table 3.

The kinematic points for which data have been obtained in SLAC E80 and in SLAC E130 are shown in Fig. 4, where proposed data points for a new experiment are also indicated.

$$\Delta = \frac{N(\uparrow\downarrow)-N(\uparrow\uparrow)}{N(\uparrow\downarrow)+N(\uparrow\uparrow)}, \quad \text{RAW ASYMMETRY}$$

$$\Delta = P_e P_p F A$$

$$A = \frac{d\sigma(\uparrow\downarrow)-d\sigma(\uparrow\uparrow)}{d\sigma(\uparrow\downarrow)+d\sigma(\uparrow\uparrow)}, \quad \text{INTRINSIC e-p ASYMMETRY}$$

$$P_e \gtrsim 0.8,\ P_p \approx 0.6,\ F \gtrsim 0.1$$

$$\Delta \approx 0.05\ A$$

COUNTING RATE VARIES FROM 0.01 TO 1/PULSE OR 1 TO 100/s.

SOURCE OF ERROR	COMMENT
COUNTING STATISTICS (Δ)	DOMINANT ERROR
	1×10^{-3} TO 3×10^{-3} IN Δ
	10% TO 30% OF Δ
P_e	$\delta P_e/P_e \sim 5\%$, MØLLER SCATTERING
P_p	$\delta P_p/P_p \sim 5\%$, NMR
F	$\delta F/F \sim 5\%$; C, CH_2 CROSS SECTIONS
RADIATIVE CORRECTIONS	WHEN COMBINED WITH COUNTING ERROR, OVERALL ERROR IS 1.1 TO 1.5 TIMES COUNTING ERROR
BACKGROUND ASYMMETRY	$\leq 1\%$ OF Δ
	MISIDENTIFIED PIONS FROM PHOTOPION PRODUCTION OFF POLARIZED PROTONS
PEGGY BEAM ASYMMETRIES	
ENERGY	$\leq 10^{-4}$ IN Δ
ANGLE	$< 10^{-4}$ IN Δ
POSITION	$< 10^{-4}$ IN Δ

2 - 81
4028A18

Table 3. Counting rates and sources of error.

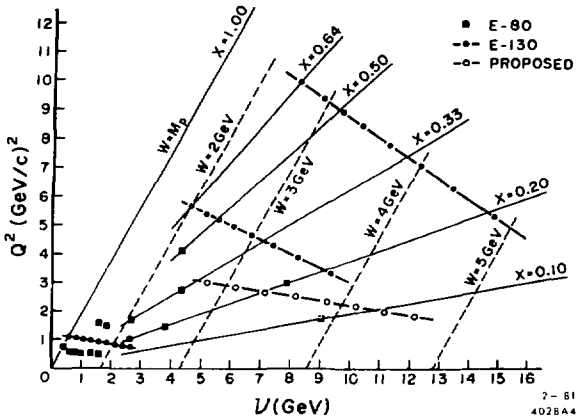

Fig. 4. Kinematic points where data have been taken.

DEEP INELASTIC DATA AND THEIR IMPLICATIONS

All the available deep inelastic asymmetry data are shown in Fig. 5, where the open diamonds are the published SLAC E80 results and the closed squares are the preliminary results for SLAC E130. The E130 results are "on-line" results, which must be checked and refined by off-line analysis. Furthermore radiative corrections are not yet included. All errors are one standard deviation total errors, which include the statistical counting error and systematic errors associated with P_e, P_p and F, added in quadrature. The new E130 data extend considerably our knowledge of the virtual photon-proton asymmetry A/D to higher Q^2 and higher x. A significant verification of the predicted scaling behavior[10] of A_1

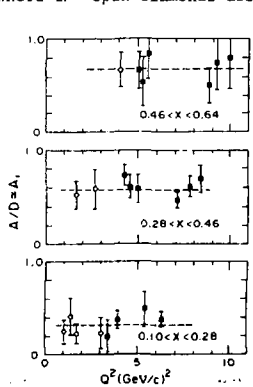

Fig. 5. Measured values of the asymmetry A/D in SLAC E80 (open diamonds) and SLAC E130 (closed squares).

$$A_1(\nu,Q^2) \to A_1(x) \text{ as } \nu, Q^2 \to \infty \text{ ; } \quad (1)$$
$$x \text{ fixed}$$

at about the 10% level over the Q^2 range from 1 to 10 $(GeV/c)^2$ is apparent from Fig. 5, where the dashed horizontal lines correspond to the average A_1 values for the three plots.

For Fig. 6 for a given x value data for different Q^2 have been combined assuming that the A/D values are independent of Q^2. These data are fit by the curve $A_1(x) = (0.90 \pm 0.05)x^{\frac{1}{2}}$.

The Bjorken sum rule is given in Eq. (2)

$$\int_0^1 \left[A_1^p F_2^p/(1+R^p) - A_1^n F_2^n/(1+R^n)\right]\frac{dx}{x} = \frac{1}{3}\left|\frac{g_A}{g_V}\right| = (0.417 \pm 0.003) \quad (2)$$

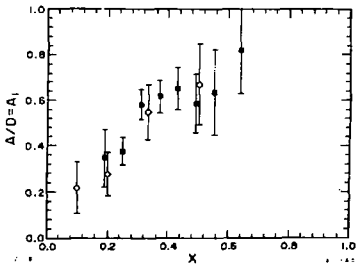

Fig. 6. Measured values of A/D vs x. Points were obtained from Fig. 5 data assuming A/D values are independent of Q^2.

in which quantities are defined in Fig. 1 and Tables 1 and 2; in addition, the superscripts p and n refer to proton and neutron, and g_V and g_A are the vector and axial vector coupling constants for neutron beta decay. The Bjorken sum rule was originally derived[11,12] from commutation relations based on the algebra of currents for the quark model. It can also be derived[13] from quantum chromodynamics (QCD) and is often written

$$\int_0^1 \left[g_1^p(x) - g_1^n(x)\right]dx = \frac{1}{6}\left|\frac{g_A}{g_V}\right| . \quad (3)$$

In the above forms the sum rule is only valid in the scaling limit.

A comparison of our data with the Bjorken sum rule is indicated in Fig. 7. Values of the quantity $A_1F_2/(1+R)$ are plotted vs x. The solid curve is a plot of the quantity $A_1F_2/(1+R)$ for the proton using the fit to our data of $A_1 = 0.90x^{\frac{1}{2}}$, $R = 0.25$ [14] and experimental values[15] of F_2 with $Q^2 = 4$ (GeV/c)^2, which is approximately the mean Q^2 for our data points. The integral under the solid curve in the range of our data from x = 0.10 to 0.64 is about 0.23

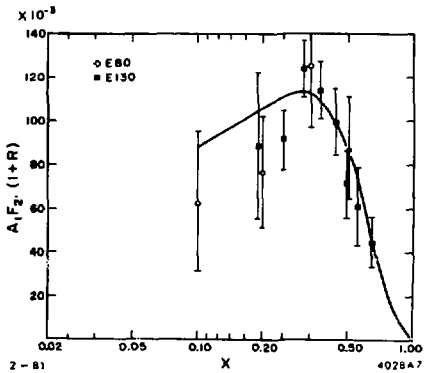

Fig. 7. Experimental values of $A_1^pF_2^p/(1+R^p)$ vs x, relevant to a test of the Bjorken sum rule.

or about 0.6 of the value predicted by the Bjorken sum rule. Clearly data at lower x are needed, and in addition an extrapolation to low x based on Regge theory can be made.[4] Since there is no experimental information about A_1 for the neutron, the neutron contribution to the integral must be ignored. Our data on A_1^p are clearly consistent with the Bjorken sum rule.

Quantum chromodynamic corrections to the Bjorken sum rule have been calculated. The leading correction in the strong coupling constant $\alpha_s(Q^2)$ is given by:[13,16]

$$\int_0^1 dx \left(g_1^p - g_1^n\right) = \frac{1}{6}\left|\frac{g_A}{g_V}\right|\left(1 - \frac{\alpha_s}{\pi}\right) \qquad (4)$$

in which $\alpha_s = [12\pi/(33-2f)]\left[\ln\left(Q^2/\Lambda^2\right)\right]^{-1}$ where f is the number of quark flavors and Λ is a free parameter. Higher order QCD corrections, including target mass effects, have also been evaluated.[17-20] Significant tests of these QCD corrections require additional experimental data as indicated below.

Another derivative form of the Bjorken sum rule due to Ellis and Jaffe[21] expresses separately a sum rule for the proton and for the neutron in the scaling limit:

$$\int_0^1 dx\ g_1^p = \left|\frac{g_A}{g_V}\right| \frac{(1.78)}{12} \quad , \qquad (5)$$

and

$$\int_0^1 dx\ g_1^n = \left|\frac{g_A}{g_V}\right| \frac{-(0.22)}{12} \quad . \qquad (6)$$

As compared to the Bjorken sum rule of Eq. (3), these sum rules involve the additional approximation that strange quarks do not contribute to the polarization asymmetry. According to Eqs. (5) and (6), the neutron contributes about 10% to the Bjorken sum rule.

Comparison of our data on A_1^p with theoretical values provides a major test for our understanding of nucleon structure. The generally accepted theory of quantum chromodynamics involving quarks and gluons has not yet been successfully applied from its own first principles to calculate either spin independent or spin dependent structure functions. However, perturbative QCD does make some important predictions about nucleon structure functions including A_1 for x near 1, which is the high momentum tail of the wave function. The models of nucleon structure[22] picture the proton as consisting of three valence quarks, two u quarks and a d quark, together with gluons and a sea of quark-antiquark pairs, and the neutron as two d quarks and a u quark together with gluons and the sea. The early models[23] assumed SU(6) symmetry for the wave function. However, experimental data on F_2^n/F_2^p and on A_1^p at large x required that SU(6) symmetry breaking be introduced. The important and unsymmetrical aspect of the wave function for the proton (neutron) near $x = 1$, which is predicted by perturbative QCD,[24] is the occurrence with high probability of a single u(d) quark with large x and a diquark with isotopic spin $I = 0$ and spin component $S_z = 0$. Of the various models for

the proton wave function which are intended to represent the nonperturbative QCD solution perhaps the most basic is the MIT bag model[22,25] which incorporates confinement.

A comparison of our data on $A_1^p(x)$ with various model predictions is shown in Fig. 8. We should remark that some earlier nonquark models of the proton predicted negative values for A_1, but all quark models predict that A_1 is positive.[3,23] Hence our earliest data indicating that A_1 is positive provided a crucial test of the quark model.[3] In the quark model A_1 can be written

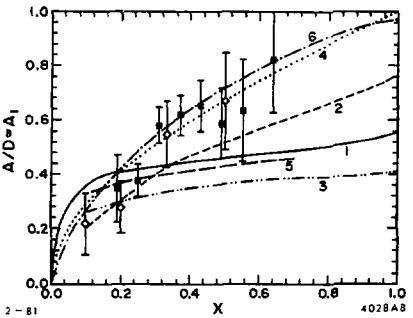

Fig. 8. Experimental values of $A/D \simeq A_1$ compared to theoretical predictions for A_1^p. The models are as follows: (1) a relativistic symmetric valence-quark model of the proton;[23] (2) a model incorporating the Melosh transformation which distinguishes between constituent and current quarks;[26] (3) a model introducing nonvanishing quark orbital angular momentum;[27,28] (4) an unsymmetrical model[29,30] in which the entire spin of the proton is carried by a single quark in the limit of $x = 1$; (5) the MIT bag model of quark confinement;[25,31] (6) source theory.[32]

$$A_1(x) = \frac{\sum_i e_i^2\left[q_i^{\uparrow} - q_i^{\downarrow}\right]}{\sum_i e_i^2\left[q_i^{\uparrow} + q_i^{\downarrow}\right]} \qquad (7)$$

in which the sum is over the quarks i, e_i is the quark i charge, and $q_i^{\uparrow}(q_i^{\downarrow})$ is the probability for quark i to have its spin parallel (antiparallel) to the target nucleon spin. A_1 clearly provides a measure of the probability that the quark spins are aligned with the nucleon spin. Only models 4 and 6 agree well with the experimental data. Curve 4 provides an unsymmetrical model of the quark distributions involving SU(6) breaking, Regge theory at small x, the Melosh transformation, and agreement with the Bjorken sum rule. Curve 6 is based on Schwinger's source theory, which is not a quark model.

RESONANCE REGION DATA AND THEIR IMPLICATIONS

The first exploratory experiment at SLAC on polarized e-p scattering in the resonance region, which was a part of E80, has recently been reported.[5] Figure 9a displays the measured asymmetry values, and Fig. 9b shows the contributions to the differential cross section from resonances and background. Our measured asymmetries A/D are predominantly large and positive throughout the entire range in missing mass W except in the region of the Δ(1232 MeV) resonance, where A/D is expected to be negative because of magnetic dipole excitation. In principle our measured asymmetry values can be predicted from a multipole analysis of complete but unpolarized electroproduction data. Figure 10 displays the predictions

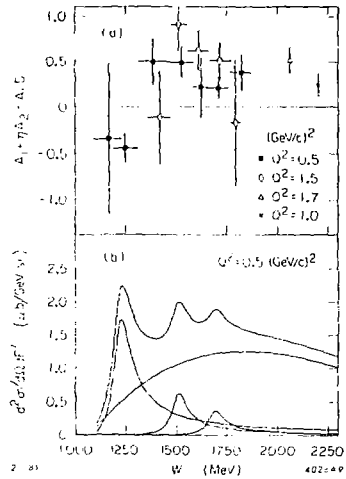

Fig. 9. (a) Asymmetry vs missing mass W. (b) Differential cross section vs W. Also shown is a decomposition into individual resonances and the background.

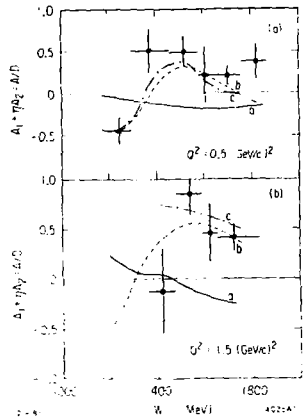

Fig. 10. (a) Asymmetry data at $Q^2 \simeq 0.5$ (GeV/c)^2 compared with a multipole analysis performed by Devenish and Gerhardt: curve a, Born terms alone; curve b, Born terms plus $\Delta(1232)$; and curve c, Born terms plus all resonances. (b) Same for $Q^2 \simeq 1.5$ (GeV/c)^2.

based on a multipole analysis of single pion electroproduction data only, which accounts for about 1/2 of the differential cross section. The agreement between these predictions and our data is rather good, and hence indicates that the net asymmetry contributed by other channels than single pion production cannot be very different from our measured asymmetries. Figure 11 indicates that scaling applies for our resonance region data except at the $\Delta(1232)$ point, and hence that the spin dependent behavior is also consistent with a global duality mechanism in analogy to the unpolarized case.

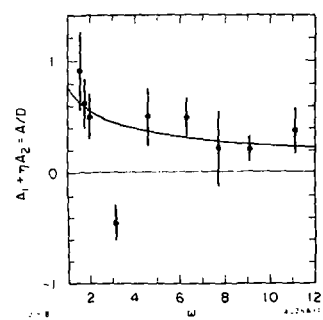

Fig. 11. Asymmetry vs scaling variable ω. The curve $0.78\omega^{-2}$ is a fit to deep-inelastic data (W > 2 GeV) of SLAC E80. The data points are the resonance-region results (W < 2 GeV) of SLAC E80.

THE FUTURE

We turn now to more futuristic aspects. An experiment[33] entitled Son of E130 has been proposed at SLAC to measure A_1 (neutron) and A_2 (proton), about which we have no experimental information. Determination of A_1^n can be done by measuring asymmetries for both the deuteron and the proton. Determination of A_2^p can be done by measuring asymmetries in scattering longitudinally polarized electrons by transversely polarized protons, and observing scattered electrons in the plane determined by the directions of the incident electron and the proton polarizations. In addition, this experiment would determine A_1^p to relatively high precision for values of x as low as 0.07. Both the data on A_1^n and the higher precision data on A_1^p at the lower x values would improve our test of the Bjorken sum rule.

Some theoretical predictions for A_1^n are shown in Fig. 12. On the basis of the spin-isospin part of the SU(6) wave function, $A_1^n = 0$ for all x (curve 1). Perhaps the most interesting prediction (curve 4) is that

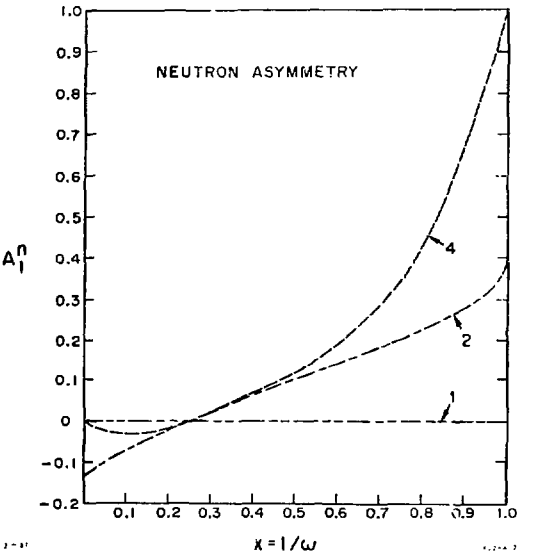

Fig. 12. Theoretical predictions for A_1 (neutron). The models are as follows: (1) a relativistic symmetric valence-quark model of the neutron;[23] (2) a model incorporating the Melosh transformation which distinguishes between constituent and current quarks;[26] (4) an unsymmetrical model[29,30] in which the entire spin of the neutron is carried by a single quark in the limit of x = 1.

of the unsymmetrical model of Carlitz and Kaur which agrees so well with the A_1^p data. It is seen that A_1^n is small over most of the range of x but becomes large at x near 1, where a single quark carries the entire spin of the neutron.

The structure function A_2 arises from an interference between amplitudes for absorption of virtual longitudinal and transverse photons by the proton.[3] In the scaling limit ν_2 becomes zero, and there is a positivity bound[34] $|A_2| < R^{\frac{1}{2}}$. Physically A_2 arises from transverse momenta of the quarks. Figure 13 shows various theoretical predictions for A_2 for the kinematics of our proposed Son of E130 experiment. The positivity limit of $|A_2| < R^{\frac{1}{2}}$ is 0.5, since the best current value[14] of R in this kinematic range is $R = 0.25 \pm 0.10$. Parenthetically, this large experimental value for R, which is expected theoretically to be zero in the scaling limit, poses a problem for QCD theory, which may be related to higher-twist terms; the comparison of theory and experiment for A_2 can be expected to pose a similar problem. In addition, Fig. 13 shows the prediction of the MIT bag model,[25,31] a prediction based on our A_1^p data together with a relation between A_1 and A_2 given by the approximate Wandzura-Wilczek sum rule,[17,35] and a prediction given from $g_2(x) = 0$ which is consistent[23] with SU(6). Data on A_2 are important for comparison with these and other[36] theories for A_2. In addition, data on A_2 are important to our experimental determination of A_1, since we measure $A/D = A_1 + \eta A_2$, and we only obtain a value of A_1 provided ηA_2 is sufficiently small. With the positivity bound for A_2, the value of ηA_2 for E80-E130 data is between 0.2 and 0.8 times the experimental one standard deviation error in our determination of A/D.

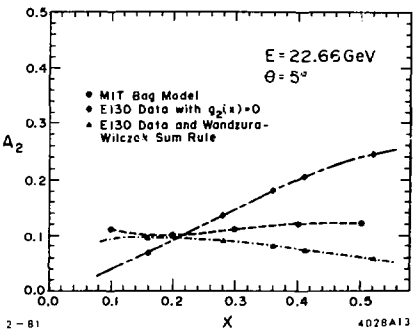

Fig. 13. Theoretical predictions for A_2 (proton) for the kinematics of the Son of E130 proposal.

Further significant tests of the scaling behavior of A_1 will only come with the availability of additional data on A_1 at higher Q^2, which is planned at CERN by the European Muon Collaboration[37] in the Q^2 range up to about 60 $(GeV/c)^2$. Figure 14 shows predictions of scaling violations of g_1 predicted[38] by QCD; they amount to about a 10% variation over the Q^2 range from 2 to 60 $(GeV/c)^2$ in the accessible range of x, and are of different sign for low and intermediate values of x. Since our measured quantity A_1 is equal to $2xg_1(1+R)/F_2$, the known scaling violations in F_2 must also be considered.

It is well known in the theory of atomic hyperfine structure[39,40] that a significant contribution to the hfs interval $\Delta\nu$ in hydrogen arises from the spin dependent polarizability of the proton. Figure 15 gives the experimental and theoretical values[41] for $\Delta\nu$. The contribution

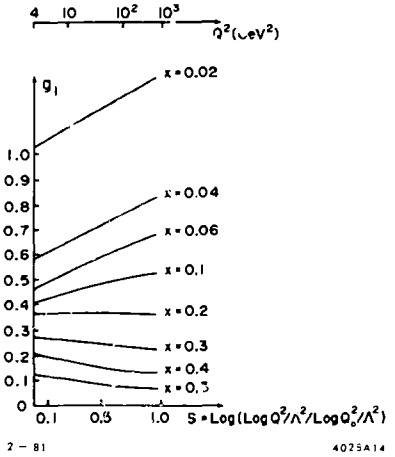

Fig. 14. Theoretical prediction[38] of scaling violation for g_1, with the parameter values $Q_0 = 2$ GeV/c and $\Lambda = 0.4$ GeV/c.

HYPERFINE INTERVAL IN HYDROGEN; EFFECT OF PROTON POLARIZABILITY

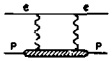

$\Delta\nu_{exp.} = 1\,420\,405\,751.766\ 7(10)$ Hz

$\Delta\nu_{theory} = \Delta\nu_F (1 + \delta_{QED} + \mu_p)$ $\quad \Delta\nu_F$ = Fermi value; δ_{QED} = QED corrections; μ_p = Proton recoil and structure term

$\delta_p = \delta_p(\text{rigid}) + \delta_p(\text{polarizability}) = -34.6(9) \times 10^{-6} + \delta_p(\text{pol})$

$$\delta_p(\text{pol}) = \frac{\alpha}{\pi}\frac{m_p}{M}\frac{1}{2(1+\mu_A)}\int_0^\infty \frac{dl(-q^2)}{(-q^2)}\left[\Delta_1(q^2) + \Delta_2(q^2)\right]$$

$$\Delta_1(q^2) = \frac{9}{4}\left[F_2(q^2)\right]^2 + 5M^2\int_{\nu_1(q^2)}^\infty \frac{d\nu}{\nu}\beta_1\left(\frac{\nu^2}{-q^2}\right)G_1(\nu,q^2)$$

$$\Delta_2(q^2) = 3M^2\int_{\nu_1(q^2)}^\infty \frac{d\nu}{\nu^2}\beta_2\left(\frac{\nu^2}{-q^2}\right)q^2\,G_2(\nu,q^2)$$

$$\beta_1(x) = \frac{8}{9}(-3x + 2x^2 + 2(2-x)\sqrt{x(x+1)});\ \beta_2(x) = 4x(1+2x-2\sqrt{x(1+x)})$$

$F_2(q^2)$ = Pauli form factor; $F_2(0) = \mu_A$; $\nu_1(q^2) = \dots + \frac{(m_\pi^2 - q^2)}{2M}$

2 - 81 4028A15

Fig. 15. Hyperfine structure interval $\Delta\nu$ in hydrogen. The Feynman diagram and the expression given for δ_p (pol) indicate the contribution of the spin dependent polarizability of the proton to $\Delta\nu$.

of the spin dependent polarizability is designated δ_p (pol). The principal theoretical uncertainty in $\Delta\nu$ is due to δ_p (pol), for which a positivity bound $|\delta_p(\text{pol})| \lesssim 3$ ppm has been calculated.[42] The quantity δ_p (pol) can be expressed[43] in terms of the spin dependent structure functions G_1 and G_2 which are measured in polarized e-p scattering. Using our experimental data for A_1^p and the Wandzura-Wilczek relation,[35] we estimate the total contribution to δ_p (pol) to be $\lesssim 0.5$ ppm from both the deep inelastic and resonance regions above a Q^2 value of ~ 5 (GeV/c)^2. The greatest contribution to δ_p (pol) comes from the small Q^2 region, including the proton resonances. Further experimental data and theoretical work should determine δ_p (pol) to a useful precision.

Finally we emphasize that knowledge of the internal spin structure of the nucleon, apart from its importance to our understanding of nucleon structure, is essential to the interpretation of spin dependent high energy phenomena involving hadrons. These include hadron-hadron scattering,[44-47] the polarized Drell-Yan process,[48,49] and production of polarized W or Z vector bosons in collisions of polarized protons in a high energy storage ring.[50,51]

REFERENCES

1. V. W. Hughes, High Energy Physics with Polarized Beams and Polarized Targets, ed. G. H. Thomas (AIP Conference Proceedings No. 51, Argonne, 1978), p. 171.
2. M. J. Alguard et al., Phys. Rev. Lett. 37, 1258 (1976).
3. M. J. Alguard et al., Phys. Rev. Lett. 37, 1261 (1976).
4. M. J. Alguard et al., Phys. Rev. Lett. 41, 70 (1978).
5. G. Baum et al., Phys. Rev. Lett. 45, 2000 (1980)
6. G. Baum et al., XXth International Conference on High Energy Physics, University of Wisconsin, July 17-23, 1980.
7. M. J. Alguard et al., Nucl. Instrum. Methods 163, 29 (1979).
8. W. W. Ash, High Energy Physics with Polarized Beams and Targets, ed. M. L. Marshak (American Institute of Physics, New York, 1976), p. 485.
9. P. S. Cooper et al., Phys. Rev. Lett. 34, 1589 (1975).
10. L. Galfi et al., Phys. Lett. B31, 465 (1970).
11. J. D. Bjorken, Phys. Rev. 148, 1467 (1966).
12. J. D. Bjorken, Phys. Rev. D1, 1376 (1970).
13. J. Kodaira et al., Phys. Rev. D20, 627 (1979).
14. L. F. Abbott et al., Phys. Rev. D22, 582 (1980).
15. A. J. Buras and K. J. F. Gaemers, Nucl. Phys. B132, 249 (1978).
16. J. Kodaira et al., Nucl. Phys. B159, 99 (1979).
17. S. Wandzura, Nucl. Phys. B122, 412 (1977).
18. J. Kodaira, Nucl. Phys. B165, 129 (1980).
19. S. Matsuda and T. Uematsu, Nucl. Phys. B168, 181 (1980).
20. C. S. Lam and B. A. Li, SLAC-PUB-2505 and 2506 (1980).
21. J. Ellis and R. Jaffe, Phys. Rev. D9, 1444 (1974).
22. F. E. Close, An Introduction to Quarks and Partons, Academic Press, London (1979).
23. J. Kuti and V. W. Weisskopf, Phys. Rev. D4, 3418 (1971).
24. G. R. Farrar and D. R. Jackson, Phys. Rev. Lett. 35, 1416 (1975).
25. R. L. Jaffe, Phys. Rev. D11, 1953 (1975).
26. F. E. Close, Nucl. Phys. B80, 269 (1974).
27. G. W. Look and E. Fischbach, Phys. Rev. D16, 211 (1977).
28. L. M. Sehgal, Phys. Rev. D10, 1663 (1974).
29. R. Carlitz and J. Kaur, Phys. Rev. Lett. 38, 673; 1102 (E) (1977).
30. J. Kaur, Nucl. Phys. B128, 219 (1977).
31. R. J. Hughes, Phys. Rev. D16, 662 (1977).
32. J. Schwinger, Nucl. Phys. B123, 223 (1977).
33. V. W. Hughes et al., SLAC Proposal Son of E130, August 1980.
34. M. G. Doncel and E. de Rafael, Nuovo Cimento 4A, 363 (1971).
35. S. Wandzura and F. Wilczek, Phys. Lett. B72, 195 (1977).
36. A. S. Joshipura and P. Roy, Phys. Lett. B92, 348 (1980).
37. E. Gabathuler, CERN Proposal by European Muon Collaboration (1974).
38. O. Darrigol and F. Hayot, Nucl. Phys. B141, 391 (1978).
39. S. J. Brodsky and S. D. Drell, Ann Rev. Nucl. Sci. 20, 147 (1970).
40. A. De Rujula et al., Phys. Lett. 33B, 605 (1970).
41. E. R. Cohen and B. N. Taylor, Jr., Phys. and Chem. Data 2, 663 (1973).
42. E. De Rafael, Phys. Lett. B37, 201 (1971).
43. R. L. Heimann, Nucl. Phys. B64, 429 (1973).
44. D. Sivers, High Energy Physics with Polarized Beams and Polarized Targets, ed. G. H. Thomas (AIP Conference Proceedings No. 51, Argonne, 1978), p. 505.

45. J. Babcock et al., Phys. Rev. D19, 1483 (1979).
46. K. Hidaka et al., Phys. Rev. D19, 1503 (1979).
47. N. Craigie et al., Phys. Lett. B96, 381 (1980).
48. J. Soffer and P. Taxil, Phys. Lett. B85, 404 (1979).
49. K. Hidaka et al., Phys. Rev. D21, 1316 (1980).
50. F. E. Paige et al., BNL-24919 (1978).
51. F. Baldracchini et al., "A Survey of Polarization Asymmetries Predicted by QCD," International Center for Theoretical Physics, Trieste, 1980.